E3S Web of Conferences **730**, 05012 (2026) https://doi.org/10.1051/e3sconf/202673005012
Soft Soils 2026

Soil arching mechanisms in piled embankments on soft soils: floating versus embedded piles

Mostafa Almasraf[1], *Araz* Salimnezhad[1], *Bedirhan Enes* Kelek[2], *S. Feyza* Cinicioglu[1*], *and Ozer* Cinicioglu[2]

[1] Department of Civil Engineering, Ozyegin University, Cekmekoy, Istanbul, Turkey
[2] Civil Engineering Department, Bogazici University, Istanbul, Turkey

Abstract. Soft soil deposits are frequently encountered along large-scale transportation infrastructure such as highways and railways. These soils pose significant challenges due to their low shear strength and high compressibility, which often lead to excessive settlements, differential deformations, and, in severe cases, structural failure. The behavior and design of piled embankments constructed over soft soils are strongly governed by the soil arching effect, which involves the redistribution of stresses between the yielding subsoil and the adjacent non-yielding zones. A piled embankment supported by end-bearing piles is considered a reliable technique for improving soft ground conditions. Nevertheless, this approach is feasible only when the compressible soil layer is relatively shallow. In regions where the soft deposit extends to considerable depths, the use of end-bearing piles becomes economically impractical. In such situations, floating (friction) piles are adopted as an alternative foundation solution. The majority of existing soil arching models are formulated to account for embedded piles. Because limited knowledge exists on how floating piles affect soil arching in piled embankments, the present study investigates this phenomenon through a series of numerical FEM analyses that compare full-scale embankments built over embedded piles with those supported by floating piles.

1 Introduction

The functionality of modern transportation networks spanning large areas depends heavily on well-engineered design practices. In geotechnical engineering, understanding the interaction between soil and structural elements is vital, especially when constructing infrastructure such as embankments, tunnels, and pipelines.

Embankments are typically constructed over soft, alluvial soils, conditions that often lead to significant settlement and deformation. To mitigate these problems, two principal construction strategies are commonly adopted. The first involves controlled staged loading to manage settlement behavior [1-3]. The second strategy involves installing piles beneath the embankment fill [4,5], which induces a load transfer phenomenon known as soil arching, a topic that has attracted increased research interest in recent years. The arching mechanism is fundamental to the behavior of CPS systems, as it controls the redistribution of stresses between the embankment fill and the much stiffer supporting piles. This mechanism is triggered by the relative movement between the soil mass and the piles.

Embankments supported by rigid inclusions, typically piles, are classified as conventional pile-supported (CPS) embankments. Compared with traditional staged construction, CPS embankments offer significant advantages in minimizing settlements and accelerating construction time [6]. Furthermore, they contribute to increased resistance against local instability and excessive deformation [7].

Two main types of pile systems are commonly used beneath embankments: embedded (end-bearing) piles and floating (friction) piles. Embedded piles transfer the embankment load directly to a competent soil layer or bedrock through the pile tip resistance [8]. However, when the soft soil layer is very thick, reaching bedrock or another strong stratum may not be feasible. In such cases, floating piles are installed, which transfer the applied loads to the surrounding soft soil primarily through shaft friction [9].

Although numerous studies have investigated piled embankments using numerical and experimental approaches, research specifically focused on arching behavior in floating-pile-supported embankments remains relatively limited. To improve understanding of the behavior of geogrid-reinforced embankments supported by floating columns, some field experiments were conducted [10]. The findings showed that settlement of the floating columns enables a redistribution of the embankment load from the columns to the surrounding soft subsoil, thereby mobilizing resistance from the underlying soil.

As floating columns penetrate deeper into the underlying soft soil under increasing construction loading, the arching efficiency progressively decreases [11]. Because floating piles undergo settlement and

* Corresponding author: feyza.cinicioglu@ozyegin.edu.tr

displacement within the soft soil, the resulting soil-structure interaction is more complex than in systems supported by end-bearing piles. Consequently, clear and unified design guidelines for floating column-supported embankments are still lacking [12]. Following the formation of the initial arching, increasing overburden load induces further relative deformation, which leads to the re-establishment of arches [13].

According to Hewlett and Randolph [14], the lateral earth pressure coefficient (K) within a piled embankment exhibits distinct states of compression and relaxation. Observing variations in K values across the embankment fill can offer valuable insights into the evolution and the mechanism of arching.

Numerous studies have explored the efficient use of piles to mobilize arching to reduce stress on the underlying subsoil. Nonetheless, questions remain about the precise mechanism of load redistribution induced by arching [15], underscoring the need for further investigation. This research investigates arching evolution and load redistribution in CPS embankments supported by embedded and floating piles, accounting for pile spacing, embankment height, and lateral earth pressure coefficients using full-scale 2D finite-element models.

2 Numerical model and material properties

The conventional pile-supported (CPS) embankments under self-weight in plane-strain 2D conditions were modeled using the finite element method (FEM)- based software, Plaxis 2D. The soil profile of Stanstead Abbots (Willow Plantation or Harlow) was selected as a well-documented case history to represent the soft ground over which the embankment will be constructed [2, 16, 17]. The soil stratigraphy and the validated geotechnical properties of Stanstead Abbotts are presented in Fig. 1 and Table 1, respectively. The groundwater is located at a depth of 1.5 m beneath the ground surface.

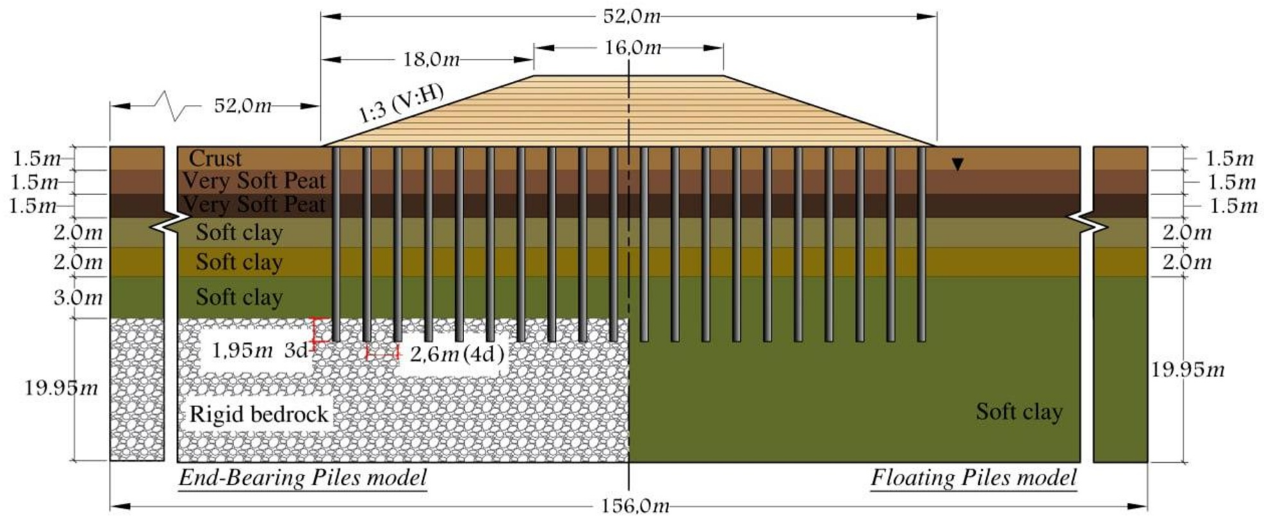

Fig. 1. Considered numerical full-scale embankment model and sub-soil.

.

Table 1. Material parameters for the piled embankment.

Material	Soil Model	Unit weight	Poisson's ratio	Permeability	Void ratio	Adopted from Hird et al. [18]		
		γ (kN/m³)	ν_{ur}	k_x=k_y (m/s)	e_0	λ^*	κ^*	ϕ' (°)
Crust	Soft Soil	16	0.15	2.5×10^{-5}	0.8	0.060	0.009	29
Very soft peat		11.4	0.15	2.5×10^{-5}	7.3	0.147	0.006	34
Very soft peat		11.4	0.15	2.5×10^{-5}	8.2	0.179	0.020	34
Soft clay		16.2	0.15	2.5×10^{-10}	1.5	0.163	0.015	28
Soft clay		16.2	0.15	2.5×10^{-10}	1.45	0.158	0.013	28
Soft clay		16.2	0.15	2.5×10^{-10}	1.4	0.060	0.009	28
Embankment fill	Hardening Soil	19	0.2	4×10^{-5}	0.5	E_{50}^{ref} (kN/m²)	E_{oed}^{ref} (kN/m²)	E_{ur}^{ref} (kN/m²)
						25×10^3	25×10^3	75×10^3
Bedrock	Mohr-Coulomb	27.5	0.3	-	0.5	E'_{ref} (kN/m²)	-	-
						4.9×10^6		
Pile	Linear Elastic	24	0.3	-	-	30×10^6	-	-

The behavior of the soft ground beneath the embankment was modeled using the Soft-Soil Model, which incorporates undrained fill construction phases followed by consolidation. Using the subsoil profile of Stanstead Abbots and adding the piles into the system, three different heights (6, 8, and 10m) were considered to analyze the behavior of the CPS piled embankments resting on the considered soil profile. The staged construction technique was adopted, with fill layer thicknesses set at 0.5m and constructed at each phase. After completion of fill construction, excess pore water pressure was allowed to dissipate during the final consolidation phase.

The angle of interface friction is taken as 2/3ϕ' by applying a 2/3 reduction factor to the shear strength angle of the soil surrounding the piles. The soil profile ends with a bedrock layer at the bottom. A pile length of 13.45 meters was kept constant between the floating and end-bearing models, where in the case of the latter one, the piles were embedded to a length of 3a into the bedrock. The pile diameters (a) are taken as 0.65m across all models. The center-to-center spacing of the piles varied as 4a, 5a, and 6a. In the floating pile-supported models, the soft soil layer was extended to a depth of 15 m below the pile tips.

2.1 Soft Soil Model Validation

The Stanstead Abbotts embankment, constructed on very soft alluvial deposits, reached a final height of 8.05 m over a period of 274 days. The staged construction sequence (Fig. 2) is simulated in the finite element (FE) analysis to accurately replicate the corresponding in-situ loading conditions. The subsurface soil profile was previously modeled by Oztoprak and Cinicioglu [2] using the Soft Soil Creep and Modified Cam Clay models. As the primary aim of the current study was to investigate the mechanism and evolution of arching, a soft soil model was adopted that accounted for the primary consolidation behavior of the soft soil layers. The soft soil model is based on the Cam-Clay model and is particularly well-suited for modeling normally and lightly over-consolidated clays, silty clays, and peat. The stress-strain response of the subsoil during construction loading was numerically derived and compared with reported stress-strain measurements for in situ, laboratory, and Mohr-Coulomb model, as well as the Soft Soil Creep model and the Soft Soil Creep model with a revised permeability coefficient (k), for validation purposes.

Fig. 2 presents a comparison between the field and laboratory vertical stress vertical-strain relationships and the finite element analysis results reported by Oztoprak and Cinicioglu [2] for the foundation soil of the Stanstead Abbotts Embankment, against the validated results obtained using the Soft Soil Model in the present study (black curve). The comparisons were performed at the midpoints of the three soil layers, denoted as (a), (b), and (c), as illustrated in Fig. 2b. The current numerical modeling approach, which incorporates staged construction conditions (showed in Fig. 2b) and employs the Soft Soil model (black curves), exhibits satisfactory agreement with the in-situ observations (dark blue curve). The stress-strain results obtained using the Soft Soil model in this study also showed good agreement with the other models, as shown in the comparative graph, except for the Mohr-Coulomb model, thereby confirming the model's reliability and providing a basis for the subsequent simulations.

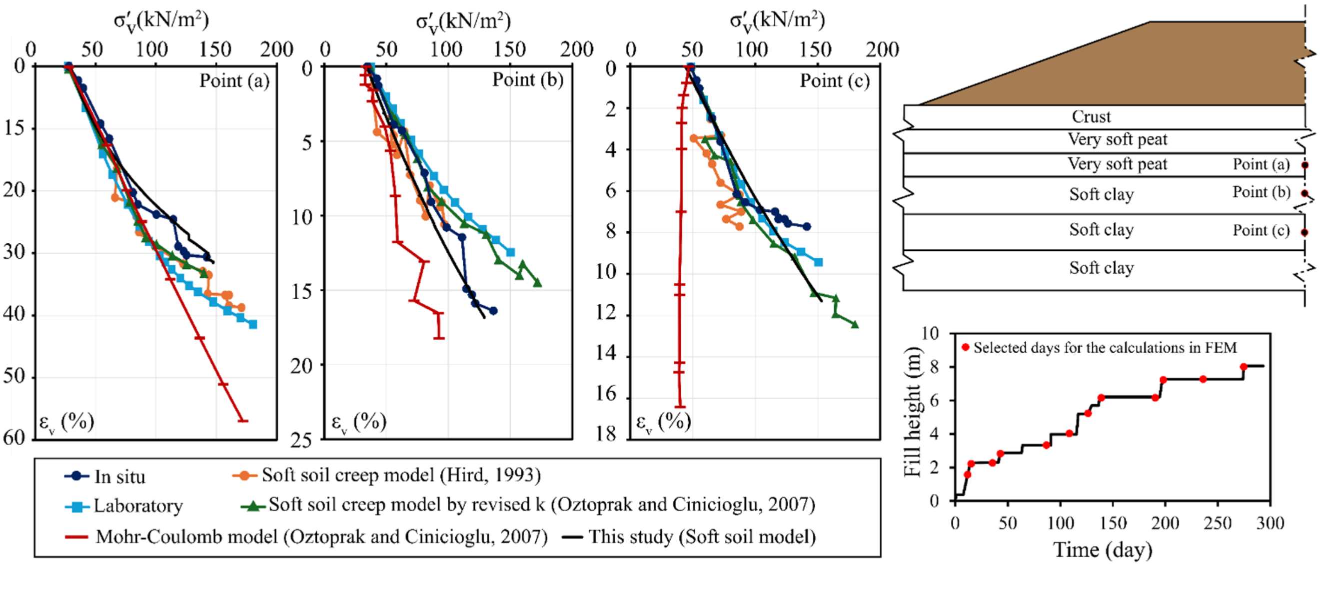

(a) (b)

Fig. 2 (a) Soft-Soil Model validation compared to experimental and numerical data, and (b) in-situ loading conditions.

https://doi.org/10.1051/e3sconf/202673005012

3 Results and discussion

3.1 Arching evolution during embankment construction

Fig. 3 and 4 show the progressive, stepwise formation and evolution of the arches within the embankment fill for the models with an 8m height and 5a pile spacing. The visible height for the study area is shown as a range from the central pile heads to 4m above them. There are 3 sets of isolines for lateral earth pressure coefficients (K). The isolines represented by shades of black correspond to the relaxation zone with 0.33<K<0.5. The compression zone (0.5<K<3) or the region where arching is formed above the subsoil due to lateral extrusion and the plugging effect of the particles is shown in shades of red. The thick red isoline represents $K_0 = 0.5$, which is the boundary of the arch separating the relaxation and compression zones. Using this novel method, not only could the precise shape and geometry of the arch be determined, but it also sheds light on the mechanical explanation of the stress redistribution in the piled embankments. Also, the shape of the isolines within the arching region is well aligned with the assumptions of the multi-shell non-concentric model by Kempfert et al. [18].

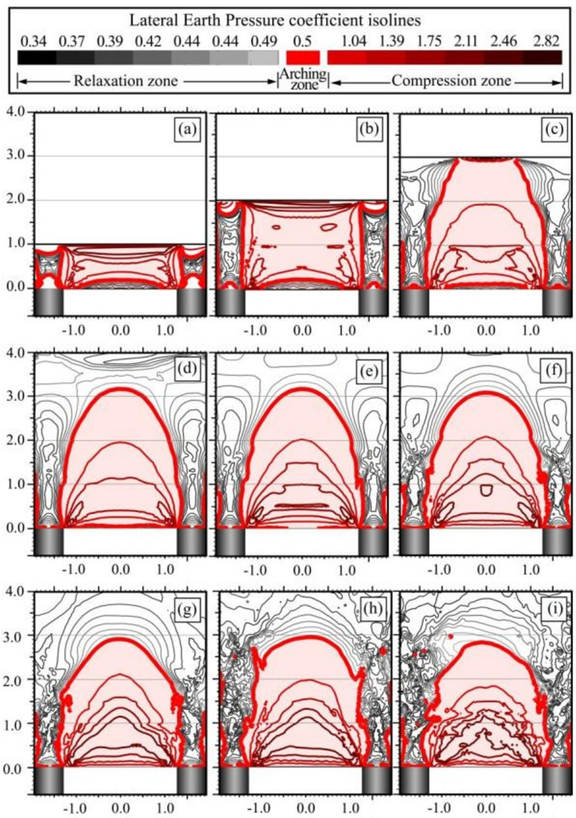

Fig. 1. Arching evolution for the embedded-pile model with an 8m height and 5a pile spacing for the fill construction heights of: (a) 1 m, (b) 2 m, (c) 3 m, (d) 4 m, (e) 5 m, (f) 6 m, (g) 7 m, (h) 8 m, and (i) Final consolidation.

For the embedded-pile-supported model, starting at 1 m, each stage shows 1 m of embankment construction, up to the final 8m height. Figs. 3 (a), (b), and (c) show that due to the insufficient height of the fill, the arching type is shear-plane arching, where the deformations in the subsoil will be directly reflected on the fill surface. However, as the fill height increases gradually, the arch starts to form and becomes a partial arch in Fig. 3d, where the arch force bridges tend to overlap above the settling subsoil. Starting from a 4m embankment height, the arch evolves from partial to full arching, and its height increases to a maximum of 3.25m (Fig. 3e). By continuing the fill construction, the overburden pressure on the arch structure increases, and as the arch remains a full arch, its height decreases to a final height of 2.8m for a fill height of 8m (Figs. 3f, 3g, and 3h). In a full arching case, the subsoil settlement will have a negligible effect on surface differential settlement in the fill.

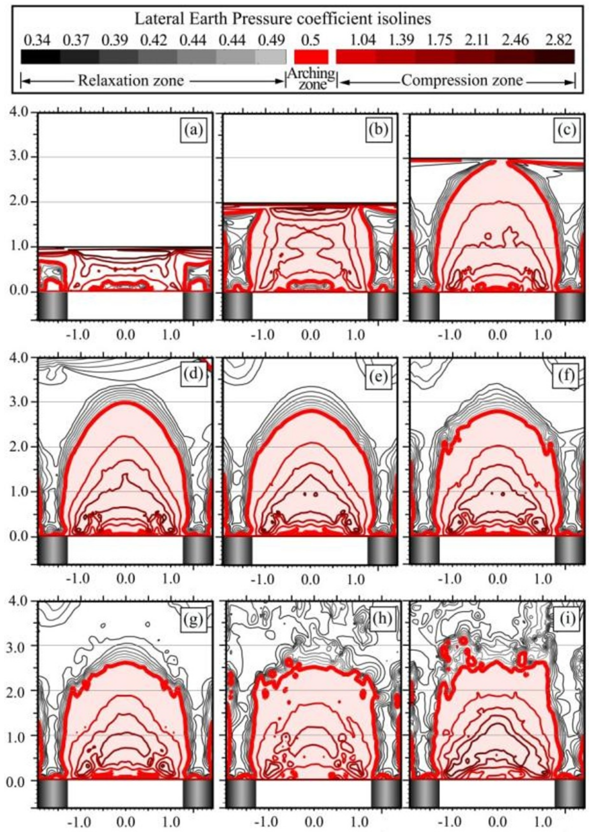

Fig. 2. Arching evolution for the floating pile model with an 8m height and 5a pile spacing for the fill construction heights of: (a) 1 m, (b) 2 m, (c) 3 m, (d) 4 m, (e) 5 m, (f) 6 m, (g) 7 m, (h) 8 m, and (i) Final consolidation.

In the case of the floating-pile-supported model, Figs. 4a and 4b show that due to the insufficient height of the fill, the arching type is shear-plane arching, as seen in the embedded model. However, as the fill height increases gradually, the arch starts to form and becomes a partial arch in Fig. 4c, where the K_0 isolines arch over the settling subsoil. In this case, the arch height is equal to the fill height. Starting from a 3m embankment height, the arch evolves from partial to full arching, and its height increases to a maximum of 3m (Fig. 4d). By continuing the fill construction, the overburden pressure on the arch structure increases, and as the arch remains a full arch, its height decreases to a final height of 2.5m for a fill height of 8m (Figs. 4h and 4i).

3.2 Stress reduction ratio (SRR) - Trapdoor physical models and piled embankments

Introduced by Low et al. [20], the stress reduction ratio (SRR) is defined as the ratio of the average vertical pressure acting on the subsoil at the clear span between two adjacent piles to the total weight of the soil column above that level. Lower SRR values indicate greater arching. At the clear spacing between the central piles, a horizontal cross-section was taken at the bottom of the fill to record the stress values throughout the construction process, from the beginning of fill construction to the end of the final consolidation phase. The mean vertical stress obtained from this cross-section represents the pressure acting on the subsoil, and, with the embankment height considered, the SRR was calculated using the following equation:

$$\text{SRR} = \sigma_v/\gamma H$$

where σ_v is the average vertical stress over the sub-soil, γ is the unit weight of the soil, and H is the embankment height.

In a trapdoor test, the trapdoor remains fixed throughout the construction of the fill and is only lowered gradually after the fill has been fully placed, allowing measurement of the acting stresses and corresponding settlements. In recent three-dimensional physical model studies, peat layers or water-saturated foam rubber cushions have been employed to simulate gradual subsoil settlement. However, unlike actual field conditions, consolidation processes during embankment construction and surcharge application were not considered. In contrast, in a real embankment, settlement of the underlying subsoil occurs from the earliest stages of fill placement. Due to this fundamental difference, the shape and evolution of SRR derived from trapdoor experiments differ significantly from those observed in real embankments. Moreover, while the trapdoor test begins from a fully loaded condition, embankment construction occurs in stages, with the load on the subsoil increasing progressively as each fill layer is placed.

Fig. 5 illustrates the variation in the stress-reduction ratio (SRR) with embankment height normalized by the clear pile spacing for embedded-pile models, considering each pile spacing. To the authors' knowledge, this study is the first to present the progressive development of soil arching and the associated redistribution of stresses between the piles and the sub-soil at each stage of embankment construction. In the graphical representation of the SRR, values greater than 1 are masked, as SRR=1 indicates no arching.

It can be seen that, for the embedded pile models (Fig. 5), the changes in SRR values at each fill height show an almost identical trend across different pile spacings. Across all pile spacings, a rapid decline in the stress reduction ratio (SRR) indicates a progressive increase in arching and a greater load transfer to the piles. In high models (10m height), beyond a certain stage, the SRR approaches an almost stable value, showing negligible variation with subsequent placement of additional fill layers. In contrast, for the 8m and especially 4 m-high embankments, the stress reduction ratio (SRR) continues to decrease throughout construction and does not reach a constant value by the time the embankment is completed, regardless of the pile spacing.

For models supported by floating piles (Fig. 6), there is no identical behavior in the SRR trends across models of the same height but with different pile spacings. It is clear that the SRR values for the floating pile models are barely reaching 0.7, indicating less efficient arching than for models supported by embedded piles, where SRR values reach 0.4.

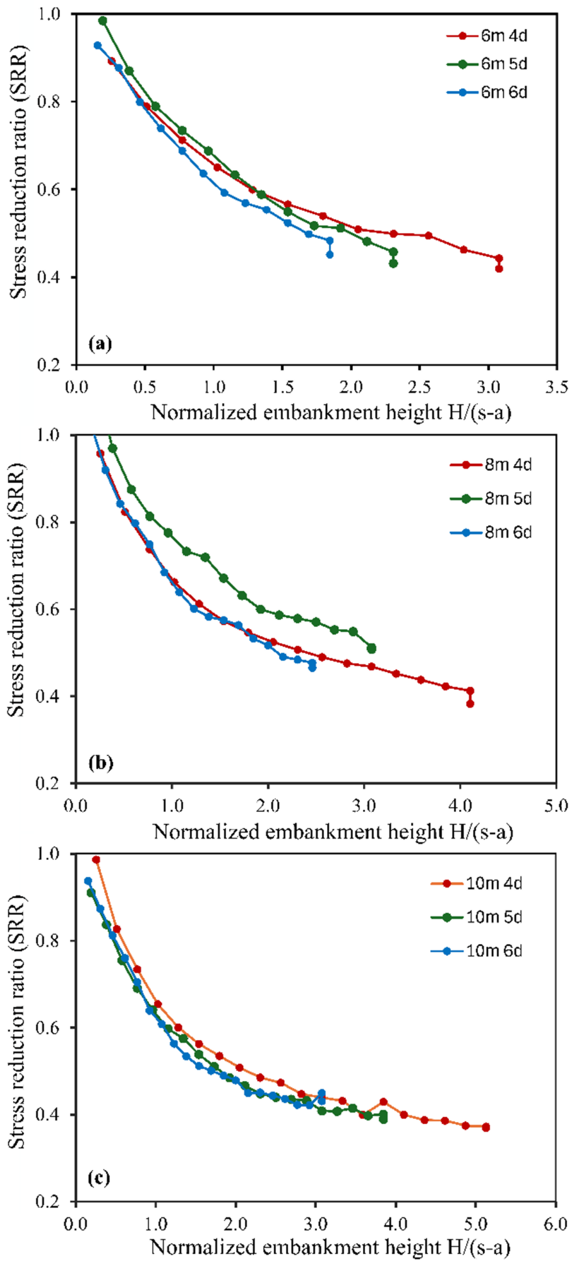

Fig. 3. SRR values at the central sub-soil span versus normalized embankment height with respect to the clear pile spacing in embedded pile models with (a) 6 m height, (b) 8 m height models, and (c) 10 m height models.

Another important point in the SRR trends of models with higher heights and larger pile spacings is the observation of an increase in SRR values following the initial decrease in the same ratio, by reaching the final phases of the fill construction. In addition, in floating pile models, final consolidation significantly reduces SRR and increases arching efficiency. Due to successive loading and higher pile settlement during fill construction, the arches degrade and reform continuously; however, during the final consolidation phase, a strong arch could form.

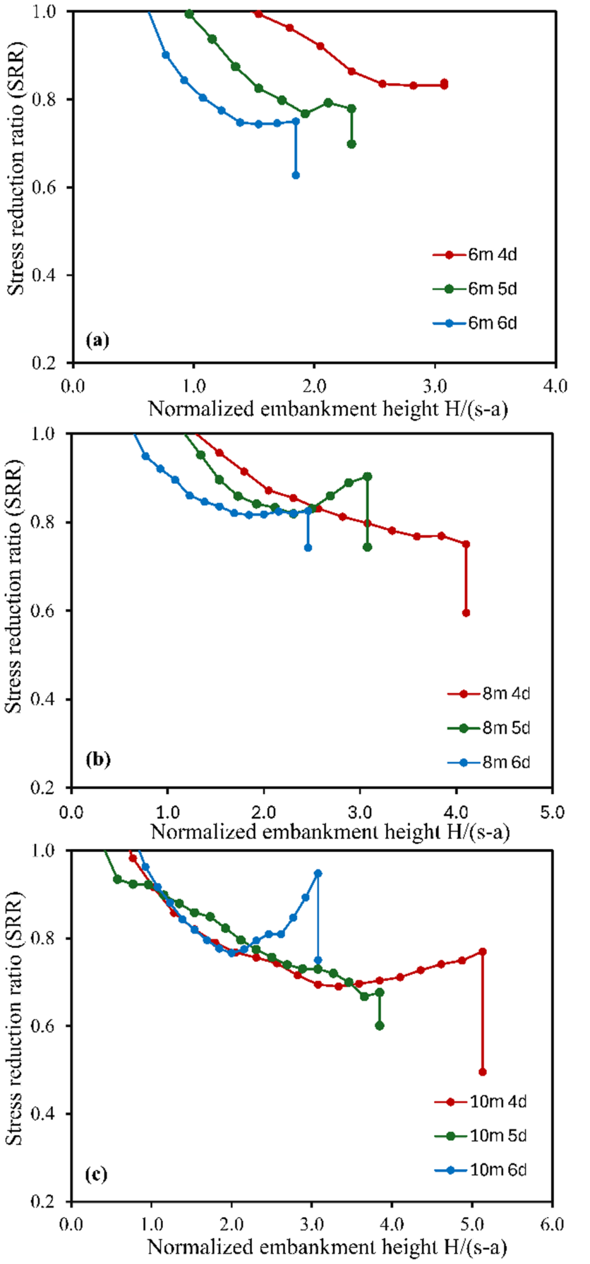

Fig. 4. SRR values at the central sub-soil span versus normalized embankment height with respect to the clear pile spacing in floating pile models with (a) 6 m height, (b) 8 m height models, and (c) 10 m height models.

4 Conclusion

Piled embankments over soft soils transfer a significant portion of the imposed embankment load to the piles through the soil arching mechanism, which redistributes stresses from yielding zones to adjacent non-yielding regions due to the stiffness contrast between pile-supported and unsupported areas. In this study, a series of full-scale FEM analyses was conducted to compare the development of soil arching in embankments supported by embedded piles and floating piles, with particular attention to the staged construction, final consolidation phase, and the evolution of the stress reduction ratio (SRR).

The results show that the development and evolution of soil arching are strongly affected by the pile support condition. During the embankment construction stages, the models supported by floating piles exhibited smaller arches compared with the embedded pile models. This indicates that the arching mechanism developed less efficiently in the floating pile systems during fill placement. This behavior was also reflected in the SRR values, where the floating pile models barely reached values of approximately 0.7, while the embedded pile models reached SRR values of about 0.4, indicating more effective stress transfer in the embedded pile-supported embankments.

However, the main difference between the two systems was not limited to the final level of arching efficiency. The SRR evolution during construction was also different. In the floating pile models, an initial decrease in SRR was followed by an increase during the final stages of fill construction. Due to successive loading and the higher settlement of the floating piles during fill placement, the arches degraded and reformed continuously.

The final consolidation phase had a significant influence on the floating pile models. Although the floating pile-supported embankments showed weaker arching during construction, final consolidation considerably reduced the SRR and increased the arching efficiency. Therefore, while the construction stages were associated with repeated degradation and reformation of arches in the floating pile models, a stronger arch could form during the final consolidation phase.

Overall, the results demonstrate that embedded and floating pile-supported embankments do not only differ in terms of their final arching efficiency, but also in terms of the way SRR evolves during construction and consolidation. Therefore, the construction-stage response, the post-construction consolidation effect, and the different SRR evolution in the two systems should be considered when evaluating soil arching in piled embankments supported by embedded and floating piles.

The authors would like to thank the Scientific and Research Council of Turkey (TUBITAK) for supporting this study with project number 122M040.

References

1. B. Indraratna, I. Sathananthan, C. Bamunawita, A.S. Balasubramaniam, Theoretical and numerical perspectives and field observations for the design and performance evaluation of embankments constructed on soft marine clay, in Elsevier Geo-Engineering Book Series, Vol. 3 (Elsevier, Oxford, U.K., 2005), pp. 51–89.
2. S. Öztoprak, S.F. Cinicioglu, Soil behaviour through field instrumentation. Can. Geotech. J. **42**, 475–490 (2005).

3. C. Öser, S.F. Cinicioglu, Embankment design method combining limit-state approach with stress-path application. Int. J. Geomech. **17**, 04016101 (2017).
4. J. Han, M.A. Gabr, Numerical analysis of geosynthetic-reinforced and pile-supported earth platforms over soft soil. J. Geotech. Geoenviron. Eng. **128**, 44–53 (2002).
5. M.K. Kelesoglu, S.F. Cinicioglu, Free-field measurements to disclose lateral reaction mechanism of piles subjected to soil movements. J. Geotech. Geoenviron. Eng. **136**, 331–343 (2010).
6. D.F. Fagundes, M.S. Almeida, L. Thorel, M. Blanc, Load transfer mechanism and deformation of reinforced piled embankments. Geotext. Geomembr. **45**, 1–10 (2017).
7. S.J.M. Van Eekelen, A.A.M. Venmans, A. Bezuijen, A.F. Van Tol, Long term measurements in the Woerden geosynthetic-reinforced pile-supported embankment. Geosynth. Int. **27**, 142–156 (2020).
8. H.G. Poulos, Design charts for piles supporting embankments on soft clay. J. Geotech. Geoenviron. Eng. **133**, 493–501 (2007).
9. S. Satibi, Numerical analysis and design criteria of embankments on floating piles, M.Sc. thesis, Inst. für Geotechnik, Univ. Stuttgart, Stuttgart, Germany, 2009.
10. W.Z. Cao, J.J. Zheng, J. Zhang, R.J. Zhang, Field test of a geogrid-reinforced and floating pile-supported embankment. Geosynth. Int. **23**, 348–361 (2016).
11. C. Xu, S. Song, J. Han, Scaled model tests on influence factors of full geosynthetic-reinforced pile-supported embankments. Geosynth. Int. **23**, 140–153 (2016).
12. T.A. Pham, K. Wijesuriya, D. Dias, Analytical model for the design of piled embankments considering cohesive soils. Geosynth. Int. **29**, 369–388 (2022).
13. C. Zhang, L. Su, G. Jiang, Full-scale model tests of load transfer in geogrid-reinforced and floating pile-supported embankments. Geotext. Geomembr. **50**, 896–909 (2022).
14. W.J. Hewlett, M.F. Randolph, Analysis of piled embankments. Int. J. Rock Mech. Min. Sci. Geomech. Abstr. **25**, 297–298 (1988).
15. S.J.M. Van Eekelen, A. Bezuijen, A.F. Van Tol, An analytical model for arching in piled embankments. Geotext. Geomembr. **39**, 78–102 (2013).
16. A. Salimnezhad, M. Almasraf, Ö. Çinioğlu, F. Çinioğlu, Comparative evaluation of arching mechanisms in low- and high-rise embankments. Turkish J. Civ. Eng. (2025), advanced online publication.
17. M. Almasraf, A. Salimnezhad, B.E. Kelek, Ö. Çinioğlu, S.F. Çinioğlu, A comparative discussion on soil arching evolution in CPS and GRPS embankments, in Geotechnical Engineering Challenges to Meet Current and Emerging Needs of Society (CRC Press, 2024), pp. 295–300. https://doi.org/10.1201/9781003431749-28.
18. C.C. Hird, I.C. Pyrah, D. Russell, S.F. Cinicioglu, Modelling the effect of vertical drains in two-dimensional finite element analyses of embankments on soft ground. Can. Geotech. J. **32**, 795–807 (1995). https://doi.org/10.1139/t95-077.
19. H.G. Kempfert, C. Göbel, D. Alexiew, C. Heitz, German recommendations for reinforced embankments on pile-similar elements, in Proceedings of the 3rd European Geosynthetics Conference, EUROGEO 3, Munich, Germany (2004), pp. 279–284.
20. B.K. Low, S.K. Tang, V. Choa, Arching in piled embankments. J. Geotech. Eng. **120**, 1917–1938 (1994).